Received: 11 September 2023 | Revised: 10 November 2023 | Accepted: 6 December 2023

DOI: 10.1111/aor.14698

Artificial Organs WILEY

MAIN TEXT

Investigation of the role of von Willebrand factor in shear-induced platelet activation and functional alteration under high non-physiological shear stress

Dong Han[1] | **Wenji Sun**[1] | **Kiersten P. Clark**[1] | **Bartley P. Griffith**[1] | **Zhongjun J. Wu**[1,2]

[1]Department of Surgery, University of Maryland School of Medicine, Baltimore, Maryland, USA

[2]Fischell Department of Bioengineering, A. James Clark School of Engineering, University of Maryland, College Park, Maryland, USA

Correspondence
Zhongjun J. Wu, Department of Surgery, University of Maryland School of Medicine, Baltimore, MA, USA.
Email: zwu@som.umaryland.edu

Funding information
National Institutes of Health

Abstract

Background: von Willebrand factor (vWF) plays a crucial role in physiological hemostasis through platelet and subendothelial collagen adhesion. However, its role in shear-induced platelet activation and functional alteration under non-physiological conditions common to blood-contacting medical devices (BCMDs) is not well investigated.

Methods: Fresh healthy human blood was treated with an anti-vWF antibody to block vWF–GPIbα interaction. Untreated blood was used as a control. They were exposed to three levels of non-physiological shear stress (NPSS) (75, 125, and 175 Pa) through a shearing device with an exposure time of 0.5 s to mimic typical shear conditions in BCMDs. Flow cytometric assays were used to measure the expression levels of PAC-1 and P-Selectin and platelet aggregates for platelet activation and the expression levels of GPIbα, GPIIb/IIIa, and GPVI for receptor shedding. Collagen/ristocetin-induced platelet aggregation capacity was characterized by aggregometry.

Results: The levels of platelet activation and aggregates increased with increasing NPSS in the untreated blood. More receptors were lost with increasing NPSS, resulting in a decreased capacity of collagen/ristocetin-induced platelet aggregation. In contrast, the increase in platelet activation and aggregates after exposure to NPSS, even at the highest level of NPSS, was significantly lower in treated blood. Nevertheless, there was no notable difference in receptor shedding, especially for GPIIb/IIIa and GPVI, between the two blood groups at the same level of NPSS. The block of vWF exacerbated the decreased capacity of collagen/ristocetin-induced platelet aggregation.

Conclusions: High NPSS activates platelets mainly by enhancing the vWF–GPIbα interaction. Platelet activation and receptor shedding induced by high NPSS likely occur through different pathways.

Dong Han and Wenji Sun contributed equally to this work.

KEYWORDS

blood-contacting medical devices, non-physiological shear stress, platelet activation, platelet dysfunction, von Willebrand factor (vWF)

1 | INTRODUCTION

Blood-contacting medical devices (BCMDs) are frequently used to treat patients with cardiovascular, pulmonary, and renal diseases by replacing or supplementing the function of diseased organs. Often, a pump is required in these devices to circulate the blood. The pumping action can produce high non-physiologic shear stress (NPSS), which can damage blood and lead to severe complications. Bleeding and thrombotic events are considered the most common complications in BCMD patients.[1,2] Although survival rates of patients with advanced heart failure treated with ventricular assist device (VAD) have begun to approach those of heart transplant recipients,[3] VAD therapy has not gained widespread acceptance in clinical practice, in part because of the device-associated thrombosis and bleeding. Despite the increasing use of extracorporeal membrane oxygenation (ECMO), patients on ECMO support frequently suffer either thrombosis or bleeding or concurrently both.[4] Bleeding and thrombotic complications are closely related to hemostatic dysfunction.[2,5] Platelets play a critical role in physiological hemostasis and pathological thrombosis. NPSS is reported to have a paradoxical effect on platelets, causing concurrent platelet activation and shedding of its key adhesive receptors, for example, glycoprotein (GP) Ibα, GPVI, and GPIIb/IIIa.[6] Platelet activation and aggregation increase the risk of thrombotic complications, while excessive shedding of receptors results in weak ligand binding, which increases the risk of bleeding.

There are several theories to explain the shear-induced platelet activation. One view suggests that the binding between von Willebrand factor (vWF) and platelet's GPIbα receptors plays a vital role.[7,8] Initial globular vWF would be unfolded and elongated under shear stress, exposing its A1 domains that can bind to GPIbα receptors on platelets. The vWF–GPIbα interaction in the bloodstream can cause platelet tethering and partitioning, triggering a sequence of intracellular signals and conformational changes of the platelet GPIIb/IIIa complex.[9,10] Another view suggests that platelets under high shear stress are activated by cell lysis, releasing the agonists that are stored in the intracellular granules of platelets and erythrocytes.[11] Others also suggest that high shear stress may directly activate the GPIIb/IIIa complex, whose binding sequences are structurally hidden within the nonactivated GPIIb/IIIa receptor and are exposed only after the receptor undergoes a conformational change upon platelet activation.[12,13] The emerging mechanisms, including mechano-destruction, mechano-activation, and mechano-transduction, suggest that shear stress activates platelets by modulating their biochemical properties.[14] Recent studies have also identified a class of shear stress-sensitive channels, such as pannexin-1, that may contribute to Ca^{2+} influx in membrane patches of platelets.[15]

vWF is known to play an important role in platelet function under physiologic shear stress, but its role under different levels of shear stress may differ. vWF–GPIbα interaction was suggested to be inefficient in inducing platelet activation at wall shear stress of 6 Pa, implying the involvement of P2Y receptors in integrin mechanotransduction.[13] By contrast, vWF can be unfolded by shear stress when reaching a critical level of shear rate ($\geq$5000 s^{-1}, ~20 Pa).[16] The platelet is activated via vWF–GPIbα interaction consequently. Moreover, platelet activation and aggregation can be significantly diminished under a maximum level of wall shear rate 11 560 s^{-1} (~40 Pa) with an exposure time of ~0.54 s by adding anti-vWF or anti-GPIbα antibodies to block the vWF–GPIbα interaction in a microfluidic channel. The study indicated an essential role of vWF in both platelet activation and aggregation under moderate wall shear stresses.[17] Although this platelet shear-sensitivity via vWF-platelet binding has been known since the 1990s,[18] the precise mechanism is elusive until recent studies supported a "trigger model,"[19] wherein shear stress exerted on vWF–GPIbα binding, serving as a pulling force to the ligand-binding domain that leads to the unfolding the mechanosensory domain and subsequent platelet signaling, activation and clearance. Collagen-anchored vWF binding to GPIbα also facilitates platelet adhesion and aggregation. While platelet aggregation is dominated by GPII/bIIIa-dependent interactions under low shear rate regimes (<1000 s^{-1}, ~4 Pa), vWF-dependent interactions become increasingly dominating as shear rates increase (>10 000 s^{-1}, ~40 Pa).[20] However, the hydrodynamics in the BCMDs are harsher and more complicated. The highest level of NPSS produced in the BCMDs can reach 500 Pa; wall and bloodstream shear stress above 100 Pa is common in centrifugal blood pumps.[21] The role of vWF in platelet activation and functional alteration under BCMDs-relevant NPSS has not been fully studied.

In this study, the role of vWF in platelet activation and functional alteration under high NPSS was investigated

by inhibiting the vWF–GPIbα interaction. To block the vWF–GPIbα interaction, fresh human whole blood was treated with an anti-vWF antibody. Blood without treatment was used as the control. Then, blood was subjected to three levels of NPSS (75, 125, and 175 Pa) for a short exposure time (0.5 s) produced by a novel shearing device. Platelet activation, expression levels of key platelet adhesion receptors (GPIb, GPIIb/IIIa, and GPVI), and agonist-induced platelet aggregation were analyzed.

2 | MATERIALS AND METHODS

2.1 | Blood collection and experimental procedure

Eight healthy donors were recruited (4 males and 4 females, age range between 23 and 42 years). The blood collection was approved by the Institutional Review Board of the University of Maryland, Baltimore, and in compliance with the Declaration of Helsinki. All the donors were informed about the aim of the study and provided written informed consent. No medication was taken two weeks prior to the blood donation. A volume of 450 mL of peripheral blood was drawn from the antecubital vein into a sterile blood collection bag containing 50 mL of 3.2% sodium citrate (Medicago AB, Uppsala, Sweden). The blood hematocrit was adjusted to 32 ± 2% by adding phosphate-buffered saline (Lonza, Walkersville, MD, USA) containing 0.5% bovine serum albumin (Sigma-Aldrich, St. Louis, MO, USA). Blood viscosity was measured using a semi-micro viscometer (Cannon Instrument Company, State College, PA, USA). The inhibition of vWF–GPIbα interaction was achieved by adding the polyclonal sheep anti-human vWF antibody (Haematologic Technologies, Essex Junction, VT, USA) to the blood with a final concentration of 15 μg/mL and incubating at 37°C for 30 min without disturbing. In parallel, blood without anti-vWF antibody treatment was used as the control.

Prepared blood was loaded into a syringe and pushed by a syringe pump through a blood-shearing device (see the schematic cross-section view of the device in Figure 1). The rotor is magnetically suspended and can rotate between 500 and 5000 RPM. A narrow gap between the rotor and the housing has a uniform width of 0.165 mm and a length of 2.5 mm, allowing the device to generate Couette flow with desired shearing conditions. By adjusting the rotational speed, the desired shear stress levels (75, 125, and 175 Pa) were generated based on the measured blood viscosity (4.50 ± 0.14 cP, $n = 6$). The desired exposure time (0.5 s) was controlled with the specific constant flow rate of the syringe pump. The shearing experiment under each condition was performed in a random order and was repeated six times. Unsheared blood was served as the baseline sample.

2.2 | Western blot analysis of blood plasma

To assess the effect of the anti-vWF antibody on blocking vWF, Western blot analysis was performed on plasma samples of anti-vWF antibody-treated and untreated blood before and after NPSS exposure. Blood samples (2 mL) were centrifuged at 160*g* for 15 min at room temperature. The resulting supernate was further centrifuged

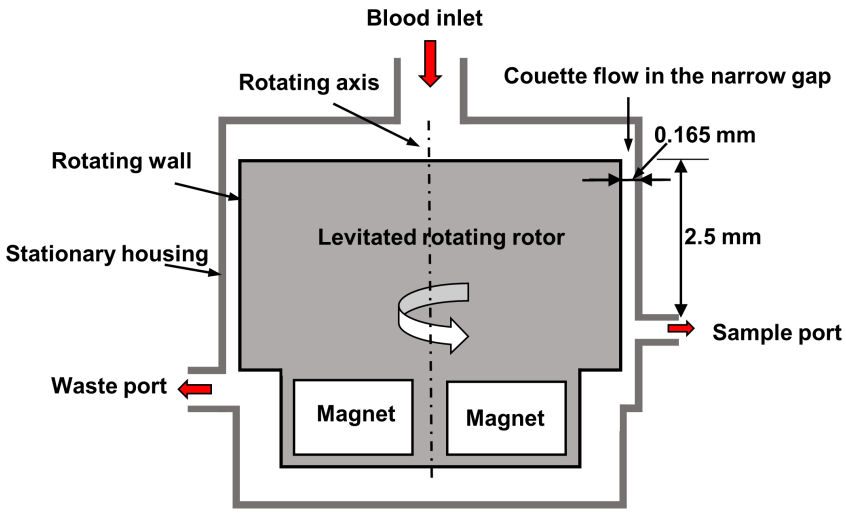

FIGURE 1 Schematic cross-section view of the blood-shearing device. Blood is sheared in the narrow gap between the levitated rotating rotor and static housing where Couette flow is generated. The level of shear stress is controlled by the rotating speed of the rotor and the exposure time is controlled by the flow rate at the blood inlet pushed by a syringe pump. Sheared blood sample is collected from the sample port, and the waste port allows excessive blood to exit. [Color figure can be viewed at wileyonlinelibrary.com]

at 14000 RPM for 10 min at 4°C to obtain platelet-poor plasma. Each plasma sample was mixed 1:20 with Laemmli sample buffer (BIO-RAD, Hercules, CA, USA). Electrophoresis was performed with agarose gel (0.6%) to separate vWF multimers. After electrophoresis, protein ladders were transferred to a nitrocellulose 0.45 μm membrane (Thermo Fisher Scientific, Waltham, MA, USA) and probed by a polyclonal rabbit anti-human vWF antibody (1:2500 dilution, Agilent Dako, Santa Clara, CA, USA), then followed by horseradish peroxidase-linked anti-rabbit IgG (1:4000 dilution). Blots were developed using Amersham ECL Western Blotting Detection Reagent (Cytiva, Marlborough, MA, USA) and scanned using ChemiDoc Imaging System (BIO-RAD).

2.3 | Flow cytometric assays for platelet activation, receptor shedding, and platelet aggregates

Platelet activation was determined by CD62P (P-Selectin) and the active GPIIb/IIIa (PAC-1). Platelet receptor shedding was quantified by measuring the expression levels of GPIbα, GPVI, and GPIIb/IIIa receptors. Blood samples (each containing 1×10^6 platelets) were added to 50 μL Tyrode's buffer with 5 mM Gly-Pro-Arg-Pro (both from Sigma-Aldrich, St. Louis, MO, USA) in 5 mL tubes and incubated with an antibody cocktail containing either 20 μL FITC-conjugated anti-PAC-1 (PAC-1-FITC, Clone PAC-1, IgM, κ), 5 μL PE-conjugated anti-CD62P (CD62P-PE, clone AK4, IgG1, κ), 5 μL PerCp-conjugated anti-CD41/CD61 antibody (CD41/CD61-PERCP, clone A2A9/6, IgG2a, κ), and 1 μL CD41a-APC (clone HIP8, IgG1, κ), or 10 μL FITC-conjugated anti-CD42b antibody (CD42-FITC, Clone HIP1, IgG1, κ), 1 μL PE-conjugated GPVI (GPVI-PE, Clone HY101, IgG1, κ), and 1 μL APC-conjugated anti-CD41a antibody (CD41a-APC, clone HIP8, IgG1, κ) at room temperature in the dark for 20 min. The corresponding isotype controls were also prepared likewise. Platelets were then fixed with 1.0 mL 1% paraformaldehyde (Affymetrix Inc, Cleveland, OH, USA) for 30 min at 4°C in the dark. FITC-labeled anti-human PAC-1, FITC-labeled anti-human CD42b, PE-labeled anti-human GPVI, and APC-labeled anti-human CD41a were purchased from BD Biosciences (San Jose, CA, USA). PerCP-labeled anti-human CD41/61 and PE-labeled anti-human CD62P antibodies were purchased from BioLegend (San Diego, CA, USA). The flow cytometry data were acquired on the BD Calibur (BD Biosciences, San Jose, CA, USA). The platelet population was identified by CD41a-APC. The expression level of P-Selectin was determined by CD62P-PE, and the expression level of PAC-1 was determined by PAC-1-FITC. The expression levels of GPIbα, GPVI, or GPIIb/IIIa were determined by CD42-FITC, GPVI-PE, or CD41/CD61-PERCP. Mean fluorescence intensity (MFI) values were calculated to represent the expression level of each marker.

Platelet aggregates were determined by the side scatter (SSC) of all CD41a positive events. CD41a-positive events were divided into two subpopulations based on the SSC-corresponded size, and the events with higher SSC were considered as platelet aggregates. 10000 CD41a-positive events were analyzed from the collected flow cytometry data.

2.4 | Platelet aggregation assay

The capacity of collagen/ristocetin-induced platelet aggregation was also evaluated using a Lumi-aggregometer (Chrono-Log, Havertown, PA, USA). A volume of 0.5 mL of each blood sample was first added into the preheated polystyrene cuvette (37°C) containing 0.5 mL saline in the aggregometer with a stir bar stirring at a speed of 1200 RPM. A volume of 5 μL collagen or 8 μL ristocetin (both from Chrono-Log) was then added to the mixed-blood sample to reach the final concentration of 4 μg/mL or 1 mg/mL, respectively. After adding agonists, the platelets started to adhere to two electrodes which would cause an increase in impedance between the electrodes. The time course of the impedance was set for 6 min. The integral of the impedance curve (area under the curve (AUC)), which indicates the overall metric for platelet aggregation, was used to represent the agonist-induced platelet aggregation capacity.

2.5 | Statistical analysis

The data were presented as mean ± standard error of the mean. Data from all blood samples were statistically analyzed by the ordinary two-way ANOVA with Sidak's multiple comparisons tests using Prism 8.4.3 software (GraphPad Software Inc., San Diego, CA, USA). A p-value <0.05 was considered statistically significant.

3 | RESULTS

3.1 | Blocking vWF

Figure 2 shows a typical image of the Western blots of vWF multimers on anti-vWF antibody-treated and untreated samples before and after NPSS exposure. The untreated samples exhibit distinct bands of vWF multimers. In contrast, samples treated with anti-vWF antibody exhibit blurred vWF blot bands, especially for high- and intermediate-molecular-weight multimers, suggesting that the vWF binding sites have been blocked by the polyclonal anti-vWF antibody.

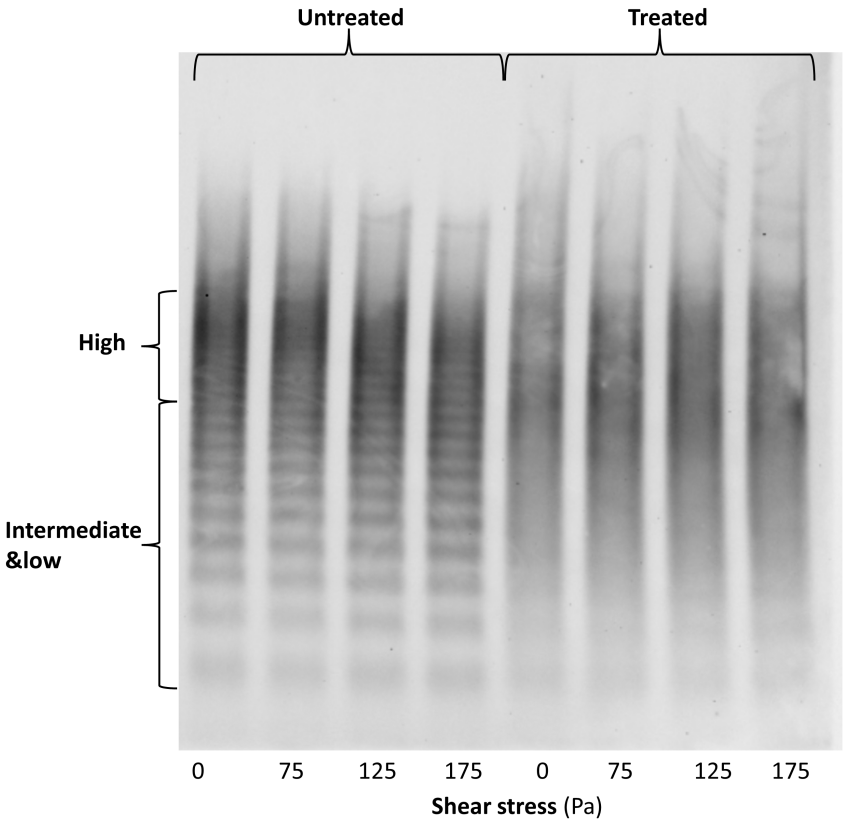

FIGURE 2 A typical image of the distribution of vWF multimers in plasma in anti-vWF antibody-treated and untreated samples, both at baseline and at three shear conditions.

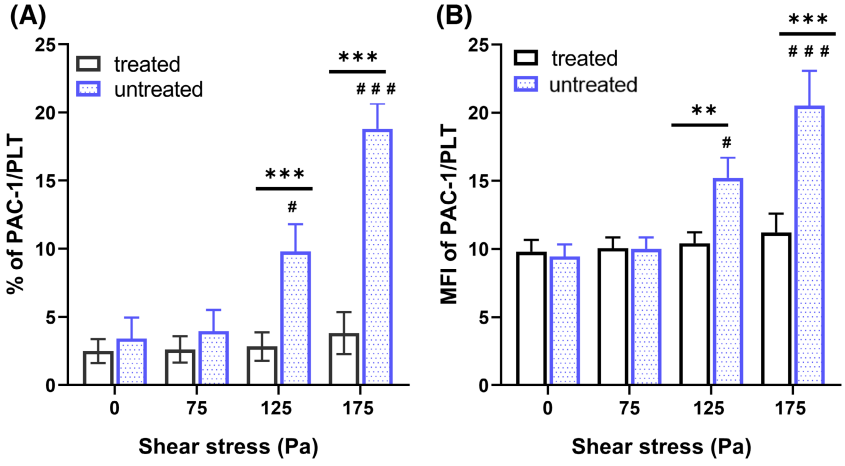

FIGURE 3 The surface expression and mean fluorescent intensity (MFI) of PAC-1 on platelets from the anti-vWF antibody-treated and untreated blood samples after NPSS exposure. (A) Percentage change of activated platelets indicated by PAC-1 surface expression. (C) MFI of activated platelets indicated by PAC-1 surface expression. (# represents the significant difference between its corresponding baseline sample, #$p<0.05$, ###$p<0.001$, $n=6$; * represents a significant difference between two groups under the same level of NPSS, **$p<0.01$, ***$p<0.001$, $n=6$). [Color figure can be viewed at wileyonlinelibrary.com]

3.2 | Platelet activation

Figure 3A shows the changes in the percentage of PAC-1^+ platelets in the blood exposed to NPSS, and Figure 3B shows the MFI of PAC-1 expression of platelets. In the untreated blood, the percentage of PAC-1^+ platelets increased from 3.42 ± 1.54% (baseline) to 3.97 ± 1.55% (75 Pa), 9.81 ± 2.01% (125 Pa), and 18.82 ± 1.84% (175 Pa). The MFI of PAC-1 expression increased from 9.46 ± 0.88 (baseline) to 10.00 ± 0.84 (75 Pa), 15.22 ± 1.50 (125 Pa), and 20.52 ± 2.55 (175 Pa). The addition of the anti-vWF antibody into the blood slightly decreased the percentage of PAC-1^+ platelets in the unsheared baseline blood sample. After being exposed to NPSS, the percentage of PAC-1^+ in the anti-vWF antibody-treated blood samples increased from 2.50 ± 0.89% (baseline) to 2.62 ± 0.97% (75 Pa), 2.84 ± 1.05%

(125 Pa), and 3.83 ± 1.54% (175 Pa), respectively. The MFI of PAC-1 expression of platelets increased slightly from 9.81 ± 0.87 (baseline) to 10.06 ± 0.79 (75 Pa), 10.42 ± 0.81 (125 Pa), and 11.21 ± 1.38 (175 Pa), respectively.

The percentage of $CD62P^+$ platelets and the MFI of CD62P expression of platelets are shown in Figure 4. The percentage of $CD62P^+$ platelets in the untreated blood samples increased from 4.26 ± 0.97% (baseline) to 5.00 ± 0.99% (75 Pa), 11.77 ± 1.52% (125 Pa), and 27.42 ± 3.37% (175 Pa) after exposed to NPSS, respectively; the MFI of CD62P expression increased from 15.98 ± 0.34 (baseline) to 16.45 ± 0.42 (75 Pa), 18.92 ± 1.20 (125 Pa), and 36.48 ± 5.72 (175 Pa), respectively. There was no notable difference in the percentage of $CD62P^+$ platelets in the baseline samples between the treated and untreated blood. After exposed to NPSS, the percentage of $CD62P^+$ in the treated blood samples increased slightly from 3.97 ± 1.24% (baseline) to 4.60 ± 1.33% (75 Pa), 5.47 ± 1.32% (125 Pa), and 7.85 ± 1.44% (175 Pa), respectively; the MFI of CD62P expression of platelets also slightly increased from 14.68 ± 0.96 (baseline) to 14.88 ± 0.83 (75 Pa), 16.03 ± 0.84 (125 Pa), and 17.62 ± 0.95 (175 Pa). Both the increases in the percentage of $PAC\text{-}1^+$ (or $CD62P^+$) and MFI of PAC-1 (or CD62P) in the treated blood samples were significantly lower than those in the untreated blood samples after being exposed to the same level of NPSS.

3.3 | Platelet receptor shedding

The MFI in the fluorescence channel for each receptor was used to represent its expression on the platelet. The baseline MFI of GPIbα, GPIIb/IIIa, and GPVI were 301.17 ± 34.63, 226.67 ± 24.54, and 297.83 ± 27.93 in the untreated blood sample, and 307.00 ± 36.03, 208.67 ± 23.33, 289.83 ± 27.40 in the treated blood sample. No significant changes were observed by *t*-test analysis for each receptor in the baseline sample after anti-vWF antibody treatment. Figure 5 shows the expression levels of the three platelet receptors after exposure to NPSS. The MFI for each receptor was normalized by its corresponding baseline MFI. A decreased level of MFI indicates loss of each receptor, that is, receptor shedding. The greater the NPSS, the more receptors were shed in both groups. In the untreated blood samples, the normalized GPIbα expression decreased to 0.93 ± 0.02-fold for 75 Pa, 0.89 ± 0.01-fold for 125 Pa, and 0.88 ± 0.01-fold for 175 Pa, GPIIb/IIIa expressions decreased to 0.92 ± 0.02-fold for 75 Pa, 0.71 ± 0.05-fold for 125 Pa, and 0.61 ± 0.07-fold for 175 Pa, and GPVI expression decreased to 0.97 ± 0.02-fold for 75 Pa, 0.93 ± 0.02-fold for 125 Pa, and 0.89 ± 0.04-fold for 175 Pa, respectively. Similarly, GPIbα, GPIIb/IIIa, and GPVI expressions in the sheared anti-vWF antibody-treated blood samples also decreased after exposure to the three levels of NPSS. In the treated blood samples with the anti-vWF antibody, GPIbα expression decreased to 0.92 ± 0.02-fold for 75 Pa, 0.84 ± 0.05-fold for 125 Pa, and 0.78 ± 0.05-fold for 175 Pa, GPIIb/IIIa expression decreased 0.94 ± 0.03-fold for 75 Pa, 0.71 ± 0.06-fold for 125 Pa, and 0.61 ± 0.06-fold for 175 Pa, and GPVI expression decreased 0.96 ± 0.01-fold for 75 Pa, 0.92 ± 0.02-fold for 125 Pa, and 0.86 ± 0.02-fold for 175 Pa, respectively. There was slightly more GPIbα receptor loss in the anti-vWF antibody-treated blood compared to the untreated blood after exposure to the same level of NPSS. No significant differences in the decreases of the GPIIb/IIIa and GPVI expressions between the untreated and treated blood after exposure to the same level of NPSS were observed.

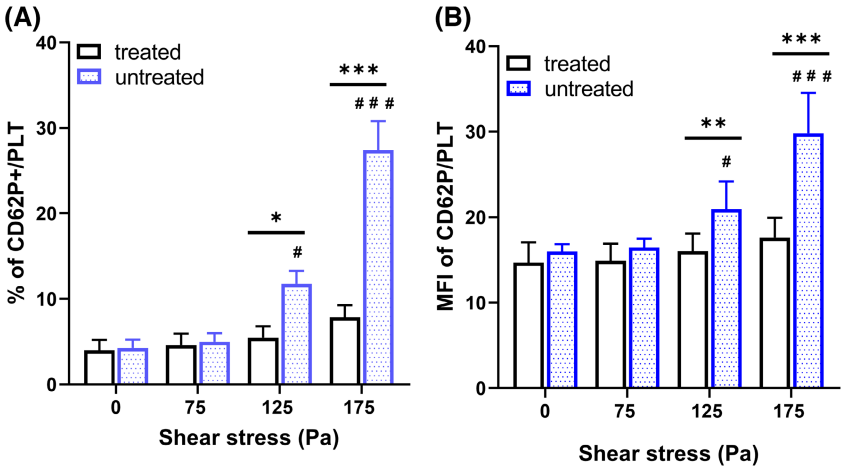

FIGURE 4 The surface expression and mean fluorescent intensity (MFI) of $CD62P^+$ on platelets from the anti-vWF antibody-treated and untreated blood after NPSS exposure. (A) Percentage change of activated platelets indicated by $CD62P^+$. (C) MFI of activated platelets indicated by $CD62P^+$ surface expression. (# represents the significant difference between its corresponding baseline sample, $\#p < 0.05$, $\#\#\#p < 0.001$, $n = 6$; * represents a significant difference between two groups under the same level of NPSS, $*p < 0.05$, $**p < 0.01$, $***p < 0.001$, $n = 6$). [Color figure can be viewed at wileyonlinelibrary.com]

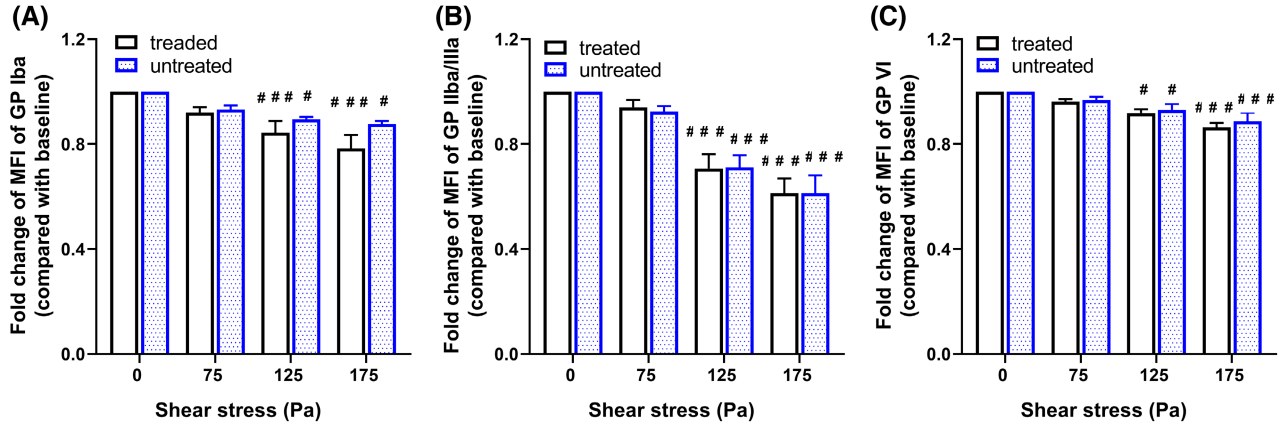

FIGURE 5 The quantification of the platelet GP receptor expression from anti-vWF antibody-treated and untreated blood after NPSS exposure. (A) Fold change of GPIbα MFI in the baseline and sheared blood samples. (B) Fold change of GPIIb/IIIa MFI in the baseline and sheared blood samples. (C) Fold change of GPVI MFI in the baseline and sheared blood samples. (# represents the significant difference between its corresponding baseline sample, #$p < 0.05$, ###$p < 0.001$, $n = 6$). [Color figure can be viewed at wileyonlinelibrary.com]

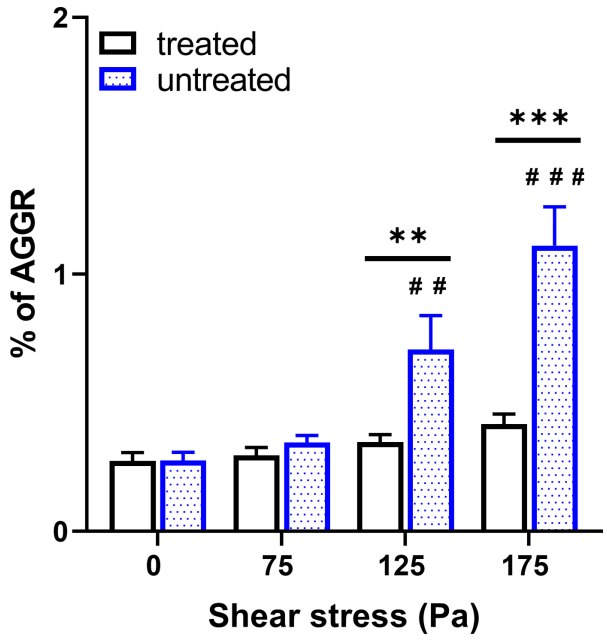

FIGURE 6 Percentage change of platelet aggregates in anti-vWF antibody-treated and untreated blood after NPSS exposure. (# represents the significant difference between its corresponding baseline sample, ##$p < 0.01$, ###$p < 0.001$, $n = 6$; * represents a significant difference between two groups under the same level of NPSS, **$p < 0.01$, ***$p < 0.001$, $n = 6$). [Color figure can be viewed at wileyonlinelibrary.com]

3.4 | Platelet aggregates

Figure 6 shows the percentage of platelet aggregates in the anti-vWF antibody-treated and untreated blood samples before and after exposure to NPSS. Consistent with platelet activation levels, the percentage of platelet aggregates significantly increased with increasing NPSS in the untreated blood. The percentage of platelet aggregates in the treated blood only slightly increased after exposure to NPSS.

3.5 | Agonist-induced platelet aggregation

Figure 7 shows typical traces of the collagen- and ristocetin-induced platelet aggregation in the vWF antibody-treated and untreated blood samples before and after exposure to NPSS. The quantity analysis of platelet aggregation capacities induced by collagen and ristocetin is shown in Figure 8. Blocking the vWF in the blood with anti-vWF antibody had a profound impact on ristocetin-induced platelet aggregation. The AUC of the ristocetin-induced platelet aggregation for the treated blood was significantly decreased compared with that for the untreated blood. The exposure to NPSS resulted in a reduction in both collagen and ristocetin-induced platelet aggregation capacities of both treated and untreated blood. The reduction in ristocetin-induced platelet aggregation capacity was more pronounced after being exposed to NPSS. The treatment with the anti-vWF antibody exacerbated these reductions, especially for the ristocetin-induced platelet aggregation capacity.

4 | DISCUSSION

Although shear stress is known to regulate platelet functions in the bloodstream, shear-induced platelet activation and functional alteration are still an open issue, especially under the uncanny non-physiological shear conditions in BCMDs. In addition to the direct impact on platelets, high

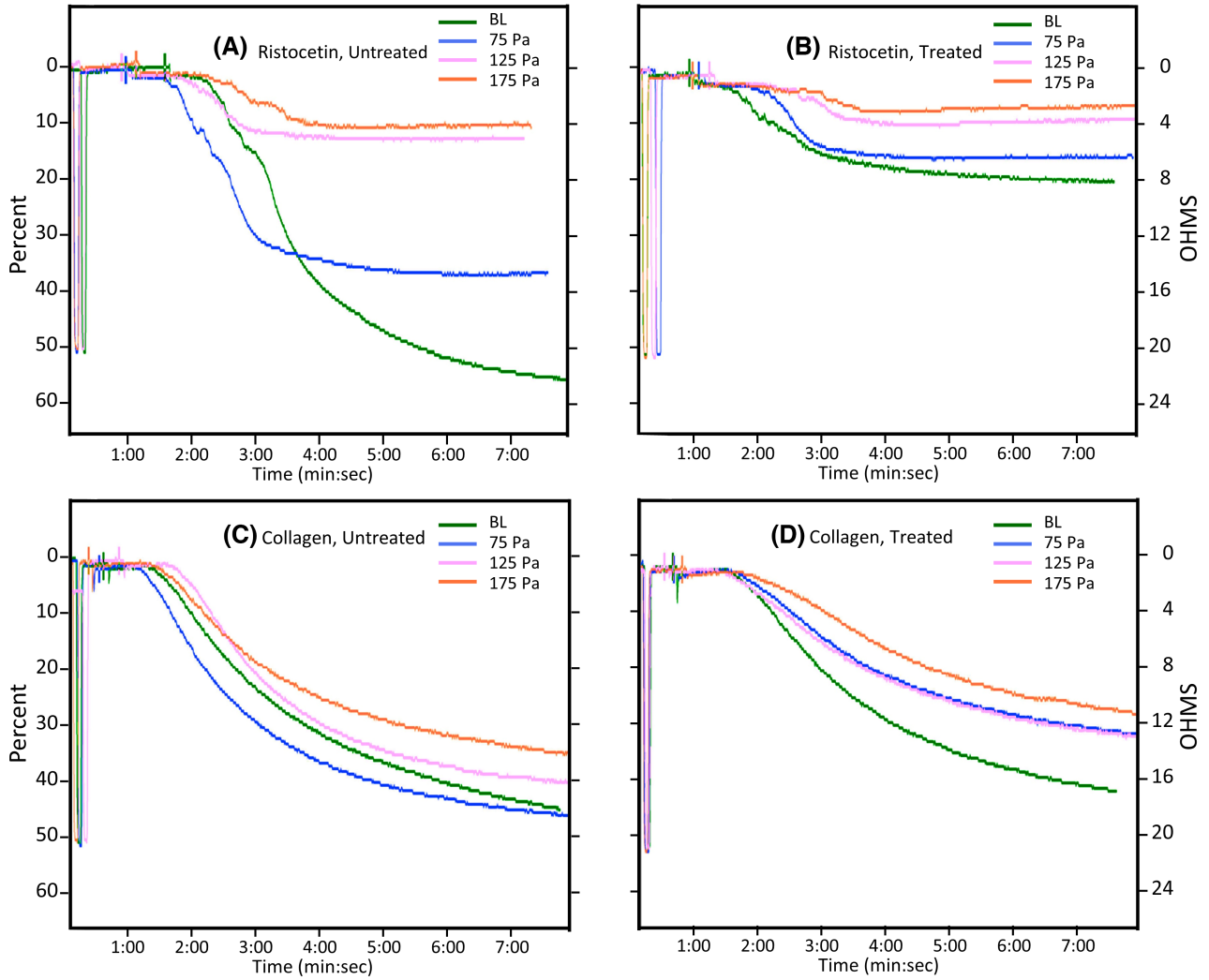

FIGURE 7 Patterns of ristocetin/collagen-induced platelet aggregation in anti-vWF antibody-treated and untreated blood after NPSS exposure. (A) Ristocetin-induced platelet aggregation for anti-vWF antibody-untreated blood. (B) Ristocetin-induced platelet aggregation for anti-vWF antibody-treated blood. (C) Collagen-induced platelet aggregation for anti-vWF antibody-untreated blood. (D) Collagen-induced platelet aggregation for anti-vWF antibody-treated blood. [Color figure can be viewed at wileyonlinelibrary.com]

shear can also damage other blood cells and plasma proteins. In the worst case, these blood components would be irreversibly ruptured, releasing cytoplasm that contains biochemical agonists such as thrombin and vWF into the bloodstream. Low shear can induce the conformational transition of vWF,[16] while high shear can deform vWF and fragment high-molecular-weight vWF multimers to intermediate or low-molecular-weight vWF multimers.[6] The shear stress threshold for shear-induced platelet activation is reported to be 50–90 Pa, whereas for vWF degradation it is around 12 Pa.[22] Degraded vWF has less affinity to platelets, which may result in decreased platelet binding capacity. It is also possible that high NPSS is too strong to break vWF–GPIbα binding.

In this study, the role of vWF in platelet activation and functional alteration under high NPSS relevant to BCMDs was investigated. The results showed that after blocking vWF in the blood, the increased levels of platelet activation and aggregates were significantly lower compared to those in the untreated blood exposed to the same levels of NPSS. Platelet activation and aggregate only showed a subtle increase even under the highest level of NPSS (Figures 3 and 4). This observation implies that high NPSS-induced platelet activation and aggregate largely require the involvement of vWF–platelet interaction. High NPSS alone may merely induce platelet activation. In previous studies using whole blood, platelet activation induced by shear stress was always concurrently accompanied by receptor shedding,[6] as was also observed in the untreated blood in this study. The greater the NPSS was, the more platelets were activated, and the more platelet receptors were shed, implying that these two trends may be correlated. Unlike the significant reduced level of platelet activation, treatment

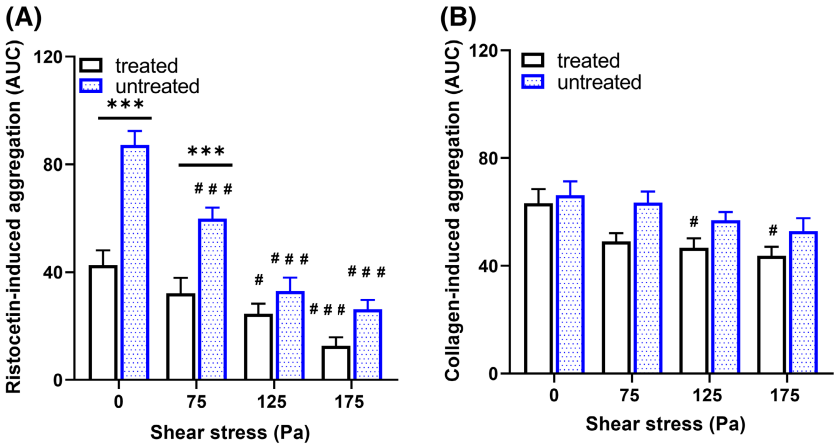

FIGURE 8 Quantification of platelet aggregation capability change (induced by collagen and ristocetin) in anti-vWF antibody-treated and untreated blood samples after NPSS exposure. The duration of the platelet aggregation curve changing was recorded for 6 min, and the platelet aggregation is indicated by AUC. (A) Change of platelet aggregation ability induced by ristocetin. (B) Fold change of platelet aggregation ability induced by collagen. (# represents the significant difference between its corresponding baseline sample, $\#p < 0.05$, $\#\#\#p < 0.001$, $n = 6$; * represents a significant difference between two groups under the same level of NPSS, $***p < 0.001$, $n = 6$). [Color figure can be viewed at wileyonlinelibrary.com]

with the anti-vWF antibody did not make a notable difference in receptor shedding, especially for GPIIb/IIIa and GPVI, compared to the untreated blood under the same level of NPSS (Figure 5). Therefore, shear-induced receptor shedding was not significantly affected by vWF and could be caused by an independent pathway that does not require platelet activation.

Blocking vWF in the blood could also significantly reduce the capacity of agonist-induced platelet aggregation. In the untreated blood, the capacities of collagen- and ristocetin-induced platelet aggregation decreased with the increasing levels of NPSS, corresponding with the loss of GPVI and GPIbα receptors on the platelet surface after exposure to NPSS. The declined capacities were exacerbated by the anti-vWF antibody treatment, especially for the ristocetin-induced platelet aggregation. vWF is related to both collagen- and ristocetin-induced platelet aggregation.[23] However, ristocetin-induced platelet aggregation mainly depends on the promotion of GPIbα-V-IX complex and vWF interaction while collagen can also induce platelet aggregation by directly interacting with GPVI.[24]

Device-associated hemostatic dysfunction remains the biggest challenge for the use and development of BCMDs. Thrombosis and bleeding account for the two devastating postsurgical complications in BCMDs-supported patients. These complications are closely associated with platelet dysfunction induced by NPSS. The development of new BCMDs urgently requires accurate numerical models for assessing platelet characteristics under complicated shear conditions. Several models have been proposed for shear-induced platelet activation, however, few considered the effect of vWF-platelet.[21] For example, numerical models based on in vitro experiments using plasma-free, gel-filtered platelets may largely underestimate the level of shear-induced platelet activation.[25] Since shear-induced platelet activation and receptor shedding may have different pathways, the numerical models for these two characteristics of platelets under NPSS should be considered separately. Therapeutics targeting shear-induced vWF A1-GPIbα interaction is a promising approach to improve the efficacy and safety profile of anti-thrombotic therapy under pathological shear circumstances.[20] Implanting this strategy may mitigate platelet activation in BCMDs, but receptor shedding may still be inevitable. To prevent platelet dysfunction caused by shear stress, the development of future BCMDs with low shear stress levels will be evident.

5 | CONCLUSION

Inhibition of vWF-platelet interaction can significantly reduce platelet activation and platelet aggregates under high NPSS, indicating that vWF plays an important role in NPSS-induced platelet activation and aggregation. NPSS induces platelet activation mainly by enhancing vWF–platelet interaction. In contrast, platelet receptor shedding showed no noticeable difference between anti-vWF antibody-treated and untreated blood samples after exposure to the same level of NPSS. Shear-induced platelet activation and receptor shedding probably have distinct pathways.

6 | STUDY LIMITATION

As vWF concentration in healthy donors' blood varies, adding the same amount of anti-vWF antibody may not completely block the vWF–platelet interaction. The concentrations of other biochemical agonists, such as adenosine diphosphate (ADP) and thrombin, in different donors, were not strictly controlled. The study examined only three NPSS conditions with a single passage (0.5 s exposure time); however, in the clinic, NPSS conditions would be more complicated. Blood would flow through the VAD/ECMO device multiple times and platelets may be sensitized during the device supporting process.[26]

AUTHOR CONTRIBUTIONS

Conceptualization, data collection & analysis, manuscript writing: Dong Han. *Conceptualization, data collection & analysis, manuscript reviewing & editing*: Wenji Sun. *Data collection & analysis*: Kiersten P. Clark. *Securing funding, manuscript reviewing*: Kiersten P. Clark. *Conceptualization, manuscript reviewing & editing, securing funding*: Zhongjun J. Wu.

ACKNOWLEDGMENTS

Research reported in this publication was supported by the National Heart, Lung, and Blood Institute of the National Institutes of Health (Award Numbers: R01HL118372, R01HL141817, and R01HL162940). The authors thank Jordan A. DeLaet for measuring collagen/ristocetin-induced platelet aggregation.

CONFLICT OF INTEREST STATEMENT

Z.J.W. and B.P.G. disclose financial interest in Abiomed/Breethe, Inc., E-Connect 1, and intellectual property for ECMO systems and blood pumps. Z.J.W. discloses serving as a consultant with Daiichi Sankyo, Inc. and CH Biomedical (USA) Inc. All other authors declare no conflict of interest in the subject matter or materials discussed in this Study.

ORCID

Zhongjun J. Wu https://orcid.org/0000-0003-0807-7195

REFERENCES

1. Mazzeffi M, Greenwood J, Tanaka K, Menaker J, Rector R, Herr D, et al. Bleeding, transfusion, and mortality on extracorporeal life support: ECLS Working Group on Thrombosis and Hemostasis. Ann Thorac Surg. 2016;101:682–9.
2. Shah P, Tantry US, Bliden KP, Gurbel PA. Bleeding and thrombosis associated with ventricular assist device therapy. J Heart Lung Transplant. 2017;36:1164–73.
3. Starling RC, Naka Y, Boyle AJ, Gonzalez-Stawinski G, John R, Jorde U, et al. Results of the post-U.S. food and drug administration-approval study with a continuous flow left ventricular assist device as a bridge to heart transplantation: a prospective study using the INTERMACS (Interagency Registry for Mechanically Assisted Circulatory Support). J Am Coll Cardiol. 2011;57:1890–8.
4. Gupta P, McDonald R, Chipman CW, Stroud M, Gossett JM, Imamura M, et al. 20-year experience of prolonged extracorporeal membrane oxygenation in critically III children with cardiac or pulmonary failure. Ann Thorac Surg. 2012;93:1584–90.
5. Chen Z, Zhang J, Kareem K, Tran D, Conway RG, Arias K, et al. Device-induced platelet dysfunction in mechanically assisted circulation increases the risks of thrombosis and bleeding. Artif Organs. 2019;43:745–55.
6. Chen Z, Mondal NK, Ding J, Koenig SC, Slaughter MS, Wu ZJ. Paradoxical effect of nonphysiological shear stress on platelets and von Willebrand factor. Artif Organs. 2016;40:659–68.
7. Reininger AJ, Heijnen HFG, Schumann H, Specht HM, Schramm W, Ruggeri ZM. Mechanism of platelet adhesion to von Willebrand factor and microparticle formation under high shear stress. Blood. 2006;107:3537–45.
8. McCrary JK, Nolasco LH, Hellums JD, Kroll MH, Turner NA, Moake JL. Direct demonstration of radiolabeled von willebrand factor binding to platelet glycoprotein Ib and IIb-IIIa in the presence of shear stress. Ann Biomed Eng. 1995;23:787–93.
9. Zlobina KE, Guria GT. Platelet activation risk index as a prognostic thrombosis indicator. Sci Rep. 2016;6:30508.
10. Chow TW, Hellums JD, Moake JL, Kroll MH. Shear stress-induced von Willebrand factor binding to platelet glycoprotein lb initiates calcium influx associated with aggregation. Blood. 1992;80:113–20.
11. Anderson GH, Hellums JD, Moake JL, Alfrey CP. Platelet lysis and aggregation in shear fields. Blood Cells. 1978;4:499–511.
12. Feng S, Lu X, Reséndiz JC, Kroll MH. Pathological shear stress directly regulates platelet αIIbβ3 signaling. Am J Physiol-Cell Physiol. 2006;291:C1346–54.
13. Goncalves I, Nesbitt WS, Yuan Y, Jackson SP. Importance of temporal flow gradients and integrin αIIbβ3 mechanotransduction for shear activation of platelets. J Biol Chem. 2005;280:15430–37.
14. Slepian MJ, Sheriff J, Hutchinson M, Tran P, Bajaj N, Garcia JGN, et al. Shear-mediated platelet activation in the free flow: perspectives on the emerging spectrum of cell mechanobiological mechanisms mediating cardiovascular implant thrombosis. J Biomech. 2017;50:20–5.
15. Taylor KA, Wright JR, Mahaut-Smith MP. Regulation of Pannexin-1 channel activity. Biochem Soc Trans. 2015;43:502–7.
16. Schneider SW, Nuschele S, Wixforth A, Gorzelanny C, Alexander-Katz A, Netz RR, et al. Shear-induced unfolding triggers adhesion of von Willebrand factor fibers. Proc Natl Acad Sci. 2007;104:7899–903.
17. Rahman SM, Hlady V. Microfluidic assay of antiplatelet agents for inhibition of shear-induced platelet adhesion and activation. Lab Chip. 2021;21:174–83.
18. Kroll MH, Heliums JD, Mclntire LV, Schafer AI, Moake JL. Platelets and shear stress. Blood. 1996;88:1525–41.

19. Deng W, Xu Y, Chen W, Paul DS, Syed AK, Dragovich MA, et al. Platelet clearance via shear-induced unfolding of a membrane mechanoreceptor. Nat Commun. 2016;7:12863.
20. Rana A, Westein E, Niego B, Hagemeyer CE. Shear-dependent platelet aggregation: mechanisms and therapeutic opportunities. Front Cardiovasc Med. 2019;6:141.
21. Han D, Zhang J, Griffith BP, Wu ZJ. Models of shear-induced platelet activation and numerical implementation with computational fluid dynamics approaches. J Biomech Eng. 2021;144:040801.
22. Chan CHH, Simmonds MJ, Fraser KH, Igarashi K, Ki KK, Murashige T, et al. Discrete responses of erythrocytes, platelets, and von Willebrand factor to shear. J Biomech [Internet]. 2022;130:110898. Available from: https://www.sciencedirect.com/science/article/pii/S0021929021006527
23. Bernardo A, Bergeron AL, Sun CW, Guchhait P, Cruz MA, López JA, et al. Von Willebrand factor present in fibrillar collagen enhances platelet adhesion to collagen and collagen-induced platelet aggregation. J Thromb Haemost. 2004;2:660–9.
24. Yoshida S, Sudo T, Niimi M, Tao L, Sun B, Kambayashi J, et al. Inhibition of collagen-induced platelet aggregation by anopheline antiplatelet protein, a saliva protein from a malaria vector mosquito. Blood. 2008;111:2007–14.
25. Nobili M, Sheriff J, Morbiducci U, Redaelli A, Bluestein D. Platelet activation due to hemodynamic shear stresses: damage accumulation model and comparison to in vitro measurements. ASAIO J. 2008;54:64.
26. Sheriff J, Bluestein D, Girdhar G, Jesty J. High-shear stress sensitizes platelets to subsequent low-shear conditions. Ann Biomed Eng. 2010;38:1442–50.

How to cite this article: Han D, Sun W, Clark KP, Griffith BP, Wu ZJ. Investigation of the role of von Willebrand factor in shear-induced platelet activation and functional alteration under high non-physiological shear stress. Artif. Organs. 2024;48:514–524. https://doi.org/10.1111/aor.14698